

Accepted Manuscript

Inhibitory effects of *N*-(acryloyl)benzamide derivatives on tyrosinase and melanogenesis

Sangwon Lee, Sultan Ullah, Chaeun Park, Hee Won Lee, Dongwan Kang, Jungho Yang, Jinia Akter, Yujin Park, Pusoon Chun, Hyung Ryong Moon

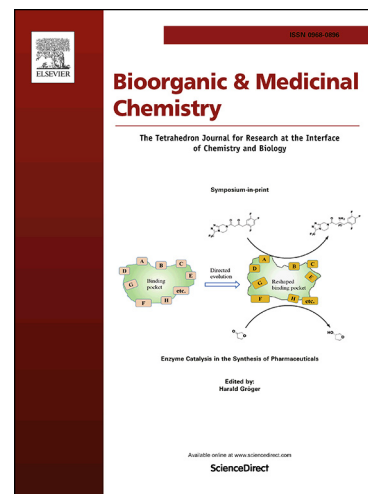
PII: S0968-0896(19)30959-9
DOI: <https://doi.org/10.1016/j.bmc.2019.07.034>
Reference: BMC 15018

To appear in: *Bioorganic & Medicinal Chemistry*

Received Date: 11 June 2019
Revised Date: 9 July 2019
Accepted Date: 19 July 2019

Please cite this article as: Lee, S., Ullah, S., Park, C., Won Lee, H., Kang, D., Yang, J., Akter, J., Park, Y., Chun, P., Ryong Moon, H., Inhibitory effects of *N*-(acryloyl)benzamide derivatives on tyrosinase and melanogenesis, *Bioorganic & Medicinal Chemistry* (2019), doi: <https://doi.org/10.1016/j.bmc.2019.07.034>

This is a PDF file of an unedited manuscript that has been accepted for publication. As a service to our customers we are providing this early version of the manuscript. The manuscript will undergo copyediting, typesetting, and review of the resulting proof before it is published in its final form. Please note that during the production process errors may be discovered which could affect the content, and all legal disclaimers that apply to the journal pertain.



**Inhibitory effects of *N*-(acryloyl)benzamide derivatives on tyrosinase and
melanogenesis**

Sanggwon Lee^{a,§}, Sultan Ullah^{a,§}, Chaeun Park^{a,§}, Hee Won Lee^a, Dongwan Kang^a, Jungho

Yang^a, Jinia Akter^a, Yujin Park^a, Pusoon Chun^b, Hyung Ryong Moon^{a,*}

^aLaboratory of Medicinal Chemistry, College of Pharmacy, Pusan National University, Busan 46241, South Korea

^bCollege of Pharmacy and Inje Institute of Pharmaceutical Sciences and Research, Inje University, Gimhae, Gyeongnam 50834, South Korea

[§]These authors (S. Lee, and S. Ullah, and C. Park) equally contributed to this work.

*Author to whom correspondence should be addressed.

Hyung Ryong Moon, Laboratory of Medicinal Chemistry, College of Pharmacy, Pusan National University, Busan 46241, Republic of Korea. *E-mail address:* mhr108@pusan.ac.kr; Tel.: +82 51 510 2815; Fax: +82 51 513 6754.

Abstract

Targeting of tyrosinase has proven to be the best means of identifying safe, efficacious, and potent tyrosinase inhibitors for whitening skin. We designed and synthesized ten NAB (*N*-(acryloyl)benzamide) derivatives (**1a** – **1j**) using the Horner-Wadsworth-Emmons olefination of diethyl (2-benzamido-2-oxoethyl)phosphonate and appropriate benzaldehydes. A mushroom tyrosinase inhibitory assay showed compounds **1a** ($36.71 \pm 2.14\%$ inhibition) and **1j** ($25.99 \pm 2.77\%$ inhibition) inhibited tyrosinase more than the other eight NAB derivatives and kojic acid ($21.56 \pm 2.93\%$ inhibition), and docking studies indicated **1a** (-6.9 kcal/mole) and **1j** (-7.5 kcal/mole) had stronger binding affinities for tyrosinase than kojic acid (-5.7 kcal/mole). At a concentration of $25 \mu\text{M}$, **1a** and **1j** were nontoxic in B16F10 melanoma cells and exhibited stronger tyrosinase inhibition (59.70% and 76.77% , respectively) than kojic acid (50.30% inhibition) or arbutin (41.78% inhibition at $400 \mu\text{M}$). Similarly, in B16F10 melanoma cells, compounds **1a** and **1j** at $25 \mu\text{M}$ decreased total melanin content by 47.97% and 61.77% , respectively (kojic acid; 38.98%). Similarities between inhibitions of tyrosinase activity and melanin contents suggested the anti-melanogenic effects of **1a** and **1j** were due to tyrosinase inhibition. The excellent DPPH scavenging activity of **1j** suggests it might enhance *in vivo* effect on melanin contents. The study suggests compound **1j** offers a potential starting point for the development of safe, potent tyrosinase inhibitors.

Key words: (*N*-(acryloyl)benzamide) derivatives, Horner-Wadsworth-Emmons olefination, melanogenesis, tyrosinase, B16F10 melanoma cells, inhibitor.

1. Introduction

Tyrosinase (EC 1.14.18.1), is a type 3, di-copper containing enzyme that produces melanin and is widely distributed in plants and animals. The tyrosinase is composed of glycoproteins and its levels are regulated by two degradation systems, that is, lysosomal/endosomal and proteasomal systems.¹ The structure of tyrosinase from *Streptomyces Castaneoglobisporus* was first determined in 2006, but other crystal structures have been reported in different species since.² Structurally, tyrosinase is composed of a central domain, a C-terminal domain and an N-terminal domain.³ The central domain consists of two copper(II) ions and six histidine residues. According to the crystal structures of tyrosinases from *Streptomyces castaneoblobisporus*, *Aspergillus oryzae*, *Agaricus bisporus*, and *Bacillus megaterium*, its central domain is responsible for its catalytic effects. The formation of a thioether bond between a cysteine residue and a histidine residue in the active site of tyrosinase stabilizes the histidine residue. Histidine is also coordinated with one of the copper ions for the catalytic mechanism. The N-terminal domain of tyrosinase determines its final shape in the presence of a transit peptide,⁴ which is responsible for melanosome transfer in mushrooms and in humans. The catalytic activity of tyrosinase is highly dependent on its two copper ions (CuA and CuB) and six histidine residues.⁵ Tyrosinase can exist in oxy, met, or deoxy forms.⁶⁻⁹ In a resting state, tyrosinase mainly exists in the met form and cannot oxidize phenols. To enable it to act as a catalyst, it must first be transformed into the deoxy form, which is readily oxidized to the oxy form. For this reason, the met form is viewed as the best target for tyrosinase inhibitors.¹⁰

Due to the ability of tyrosinase to catalyze the rate-limiting step of melanin production, it is considered an important target for the treatment of abnormal melanogenesis. Researchers have tried many approaches based on the modulation of tyrosinase expression,¹¹ maturation,^{12,13}

degradation,¹⁴ and direct catalytic activity,¹⁵ to control abnormal melanin production. However, although a large number of tyrosinase inhibitors have been identified, relatively few are used as skin lightening agents because they lack potency and have poor safety profiles.¹⁵ The skin lightening agents commonly used in the cosmetic market are hydroquinone, monobenzyl hydroquinone, arbutin,¹⁶⁻²⁰ kojic acid,²¹ salicylhydroxamic acid,²² azelaic acid,²³ and corticosteroids.^{22,23} However, the use of hydroquinone is restricted because it is cytotoxic to mammalian cells and its use is associated with serious side effects, which include skin irritation, burning, contact dermatitis, hypochromia, and chestnut spots over nails.²⁴⁻²⁷ Similarly, the use of kojic acid is restricted due to its instability and carcinogenicity.^{16,21} Furthermore, EU cosmetic regulations ban the use of hydroquinone and of corticosteroids as skin whitening agents. Thus, there is a need for safe, effective tyrosinase inhibitor for skin whitening agents.

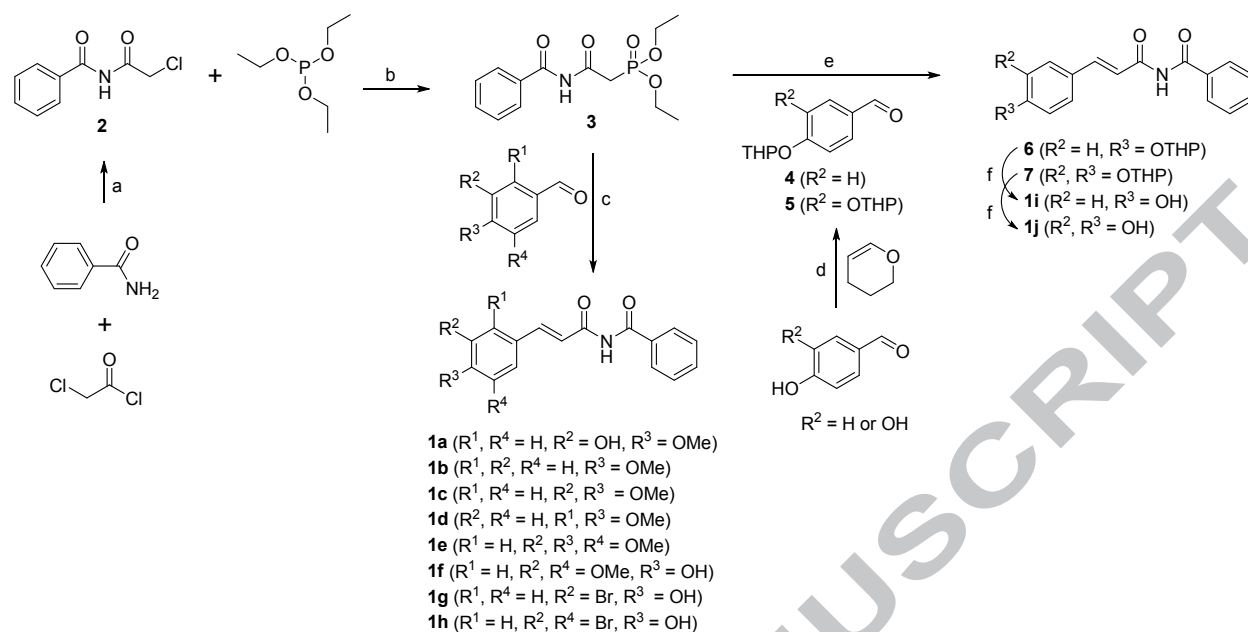
As part of our continued efforts to identify safe melanogenic materials, we synthesized a series of tyrosinase inhibitors and found that compounds possessing the (*E*)- β -phenyl- α,β -unsaturated carbonyl motif showed excellent tyrosinase inhibitory activity. Analogues containing the (*E*)- β -phenyl- α,β -unsaturated carbonyl motif have also been reported to have many different biological activities including anticancer agents,²⁸ anti-convalescent agents,²⁹ anti-oxidant agents,³⁰ anti-viral agents,³¹ and anti-malarial agents.^{32,33} The natural substrates of tyrosinase are L-tyrosine and L-dopa, which have hydroxyl groups on their phenyl ring. The hydroxyl groups may play an important role in binding to the tyrosinase enzyme. Therefore, we want to introduce different substituents such as hydroxyl, methoxyl, and bromo groups to the β -phenyl ring of the carbonyl motif and to compare the effects of the substituents on tyrosinase inhibition. For this purpose, *N*-(acryloyl)benzamide (NAB) derivatives,³⁴⁻³⁷ which also contain the (*E*)- β -phenyl- α,β -unsaturated carbonyl motif, were synthesized as potential tyrosinase inhibitors, and evaluated with respect to

their abilities to inhibit mushroom tyrosinase, and tyrosinase activity and melanin production in B16F10 melanoma cells.

2. Results and discussions

2.1. Chemistry

A strategy for the preparation of NAB derivatives is depicted in Scheme 1. It was envisioned that NAB derivatives could be produced by condensation between diethyl (2-benzamido-2-oxoethyl)phosphonate (**3**) and appropriate benzaldehydes. Reaction between benzamide and chloroacetyl chloride gave *N*-acyl benzamide **2**³⁸ in 58% yield, and subsequent reaction between **2** and triethyl phosphite afforded phosphonate **3**³⁸ a key intermediate for the synthesis of NAB derivatives by Michaelis-Arbuzov rearrangement. To synthesize NAB derivatives **1i** and **1j**, which contain a 4-hydroxyphenyl or a 3,4-dihydroxyphenyl, respectively, the hydroxyl groups of 4-hydroxybenzaldehyde and 3,4-dihydroxybenzaldehyde were first protected with a tetrahydropyranyl (THP) ether using 3,4-dihydro-2*H*-pyran in the presence of pyridinium *p*-toluenesulfonate to afford compounds **4** (90.9%) and **5** (79.7%), respectively. Horner-Wadsworth-Emmons olefination³⁹ of phosphonate **3** with different substituted benzaldehydes produced the desired NAB derivatives **1a** – **1h** and the THP-protected NAB derivatives **6** and **7**. These two derivatives were deprotected under acidic conditions using 2M-HCl in 1,4-dioxane to give the NAB derivatives **1i** and **1j**. The structures of NAB derivatives **1a** – **1j** were confirmed by ¹H and ¹³C NMR and high resolution mass spectrometry.

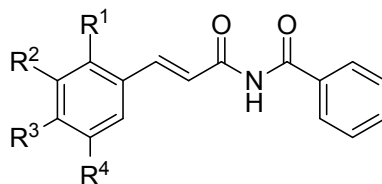


Scheme 1. Synthetic scheme for NAB derivatives **1a** – **1j**. Reagents and conditions: a) reflux, 50 min, 58%; b) 80 °C, 24 h, 51%; c) NaH, THF, rt, 1 – 12 h, 26 – 86%; d) pyridinium *p*-toluenesulfonate, DCM, rt, 2 – 50 h, 91% for **4**, and 80% for **5**; e) NaH, THF, rt, 3 h, 69% for **6**, and 88% for **7**; f) 2M-HCl, 1,4-dioxane, rt, 30 min, 63% for **1i**, 6 h, 49% for **1j**.

2.2. Mushroom tyrosinase inhibition assay for NAB derivatives **1a** – **1j**

Mushroom tyrosinase inhibitions by NAB derivatives **1a** – **1j** were determined at a concentration of 25 μ M, and kojic acid (25 μ M; a well-known tyrosinase inhibitor) was used as the control. Results are summarized in Table 1. Although all NAB derivatives harboured the β -phenyl- α,β -unsaturated carbonyl motif, the types and positions of substituents on the β -phenyl ring of NAB derivatives were found to greatly influence their activities. Among the four NAB derivatives with a β -3,4-disubstituted-phenyl ring, compound **1a** with a 3-hydroxy-4-methoxyphenyl ring and compound **1j** with a 3,4-dihydroxyphenyl ring showed greater tyrosinase inhibitory activity (36.71 ± 2.14 and $25.99 \pm 2.77\%$, respectively) than kojic acid ($21.55 \pm 2.30\%$). On the other hand, NAB derivatives (**1c** – **1e**) either failed (**1e**) or only weakly inhibited tyrosinase ($5.49 \pm 2.21\%$ for **1c**, $8.05 \pm 2.84\%$ for **1d**). Compound **1b** did not have a hydroxyl group like **1c** – **1e** but

moderately inhibited tyrosinase activity by $17.14 \pm 3.94\%$. Derivative **1i**, which possessed a 4-hydroxyphenyl ring, also potently inhibited tyrosinase (by $19.18 \pm 1.14\%$). Notably insertion of a hydroxyl group into position 3 of the β -phenyl ring of **1i** increased inhibitory activity (**1i**: $19.18 \pm 1.14\%$ vs. **1j**: $25.99 \pm 2.77\%$), whereas the insertions of methoxyl groups into positions 3 and 5 greatly diminished inhibitory activity (**1i**: $19.18 \pm 1.14\%$ vs. **1f**: $5.54 \pm 2.35\%$). The additional introduction of bromo groups into positions 3 and/or 5 also reduced inhibitory activity (**1i**: $19.18 \pm 1.14\%$ vs. **1g**: $11.32 \pm 2.90\%$ and **1h**: no inhibition). These results suggest the β -phenyl- α,β -unsaturated carbonyl motif plays a key role in the inhibition of tyrosinase and that substituent type and location on the β -phenyl ring sensitively affect tyrosinase inhibition.

Table 1. Inhibitory effects of NAB derivatives **1a** – **1j** and of kojic acid on mushroom tyrosinase

| Compound | R ¹ | R ² | R ³ | R ⁴ | Tyrosinase inhibition (%) |
|------------|----------------|----------------|----------------|----------------|---------------------------|
| 1a | H | OH | OMe | H | 36.71±2.14 |
| 1b | H | H | OMe | H | 17.14±3.94 |
| 1c | H | OMe | OMe | H | 5.49±2.21 |
| 1d | OMe | H | OMe | H | 8.05±2.84 |
| 1e | H | OMe | OMe | OMe | ^a NI |
| 1f | H | OMe | OH | OMe | 5.54±2.35 |
| 1g | H | Br | OH | H | 11.32±2.90 |
| 1h | H | Br | OH | Br | NI |
| 1i | H | H | OH | H | 19.18±1.14 |
| 1j | H | OH | OH | H | 25.99±2.77 |
| Kojic acid | | | | | 21.55±2.30 |

Tyrosinase inhibitions were measured at a derivative concentration of 25 μ M. L-Tyrosine was used as a substrate. Results are expressed as means \pm SEMs. ^aNI: no inhibition

2.3. Docking simulation study of derivatives **1a** and **1j**

To investigate interactions with tyrosinase at the molecular level, docking simulations were performed using NAB derivatives **1a** and **1j**, which most inhibited mushroom tyrosinase. We used AutoDock Vina 1.1.2 docking software developed by the Scripps Research Institute for the

simulations. Using the energy minimization tool of Chem3D Pro 12.0 software from CambridgeSoft Corporation, we created stable 3D structures of ligands **1a** and **1j**. The structure of mushroom tyrosinase was obtained from the Protein Data Bank (ID: 2Y9X). As shown in Figure 1d, ligands **1a** and **1j** showed stronger binding affinities for tyrosinase (-6.4 and -7.5 kcal/mole, respectively) than kojic acid (-5.7 kcal/mole). To investigate the natures of binding interactions, we used a LigandScout 4.3.0 software to produce pharmacophore models. As shown in Figure 1b, kojic acid interacted with amino acid His263 by π - π stacking and formed two hydrogen bonds with the amino acid residues of His259 and His263. The ligand **1a** interacted hydrophobically with the tyrosinase amino acids Val248, Met257, Phe264, and Val283. On the other hand, compound **1j** interacted hydrophobically with Val248, Phe264, and Val283. These results indicate the **1a** and **1j** bind strongly to tyrosinase at its active site.

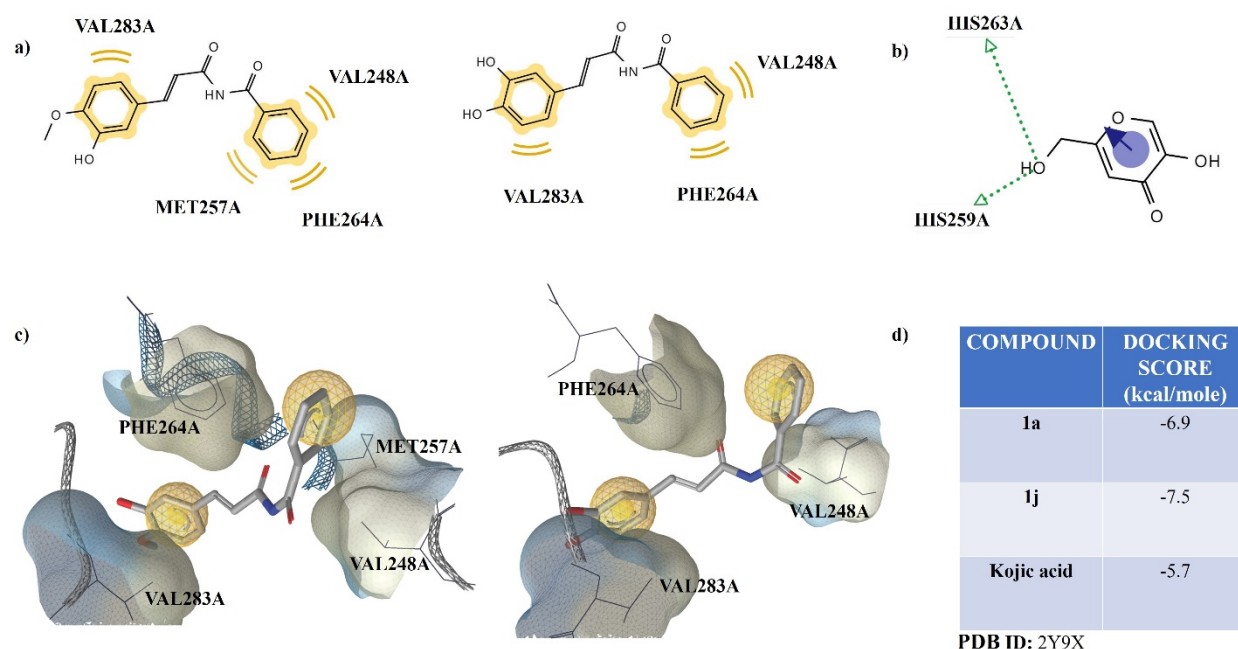


Figure 1. Binding scores and interactions of NAB derivatives **1a** and **1j** and kojic acid with tyrosinase. (a, and b) Pharmacophore results for **1a** and **1j** and kojic acid obtained using LigandScout 4.3.0 showed probable hydrogen-bonding (green arrows), π - π stacking (violet

arrow), and hydrophobic interactions (yellow) between **1a**, **1c**, and kojic acid and amino acid residues of tyrosinase, (c) 3D pharmacophore models of ligands **1a** and **1j** and tyrosinase, and (d) binding scores for interactions between ligands **1a**, **1j**, and kojic acid and tyrosinase.

2.4. Cytotoxicities of NAB derivatives **1a** and **1j**

Derivatives **1a** and **1j** were chosen for the cytotoxicity study, which was performed using a WST-8 assay. NAB derivatives **1a** and **1j** were prepared at concentrations of 0, 5, 10, and 25 μM and treated with B16F10 melanoma cells in an incubator for 24 h. As shown in Figure 2, neither derivative exhibited a cytotoxic effect at concentrations up to 25 μM . Thus, further studies on the anti-tyrosinase and anti-melanin production activities of **1a** and **1j** were conducted at concentrations $\leq 25 \mu\text{M}$ in B16F10 melanoma cells.

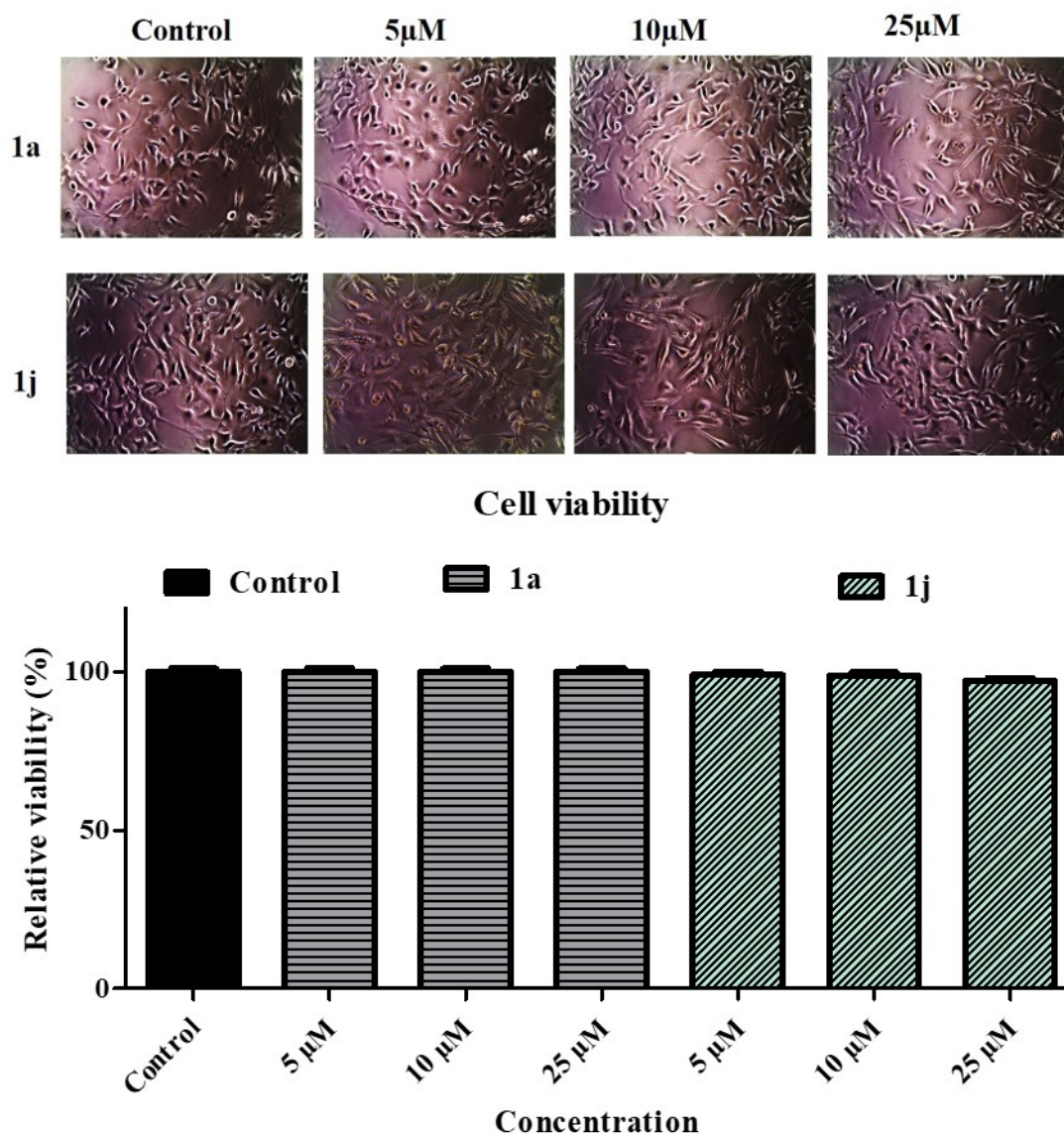


Figure 2. Cytotoxic effects of NAB derivatives **1a** and **1j** in B16F10 melanoma cells at concentrations of 5, 10, or 25 μM . Cytotoxic effects are expressed as percentage viabilities versus non-treated controls. Standard errors are indicated by bars.

2.5. Mammalian tyrosinase inhibition by NAB derivatives **1a** and **1j** in B16F10 cells

B16F10 melanoma cells were stimulated with α -MSH hormone and treated with **1a** or **1j** at concentrations of 0, 5, 10, or 25 μM , kojic acid (25 μM), or arbutin (400 μM ; positive control)

and cellular tyrosinase activities were screened. Cells were incubated in a 5% CO₂ environment for 24 h. Results were obtained by measuring optical densities.

As shown in Figure 3, NAB derivatives **1a** and **1j** inhibited tyrosinase more potently than kojic acid or arbutin. At a concentration of 25 μ M, **1a** (59.70% inhibition) more strongly inhibited tyrosinase than kojic acid (50.30% inhibition) or arbutin (41.78% inhibition). **1j** (76.77% inhibition) with a 3,4-dihydroxyphenyl ring at the β -position of the α,β -unsaturated carbonyl motif inhibited tyrosinase more at this concentration than **1a**, which conflicted with our mushroom tyrosinase results. We attribute this to structural differences between mushroom tyrosinase and the mammalian tyrosinase of B16F10 melanoma cells. Both **1a** and **1j** induced significant decreases in tyrosinase activities at all concentrations tested versus non-treated controls, and inhibited tyrosinase activity in a concentration-dependent manner. These results suggest that the (*E*)- β -phenyl- α,β -unsaturated carbonyl motif plays an important role in the inhibitions of mushroom and mammalian tyrosinase.

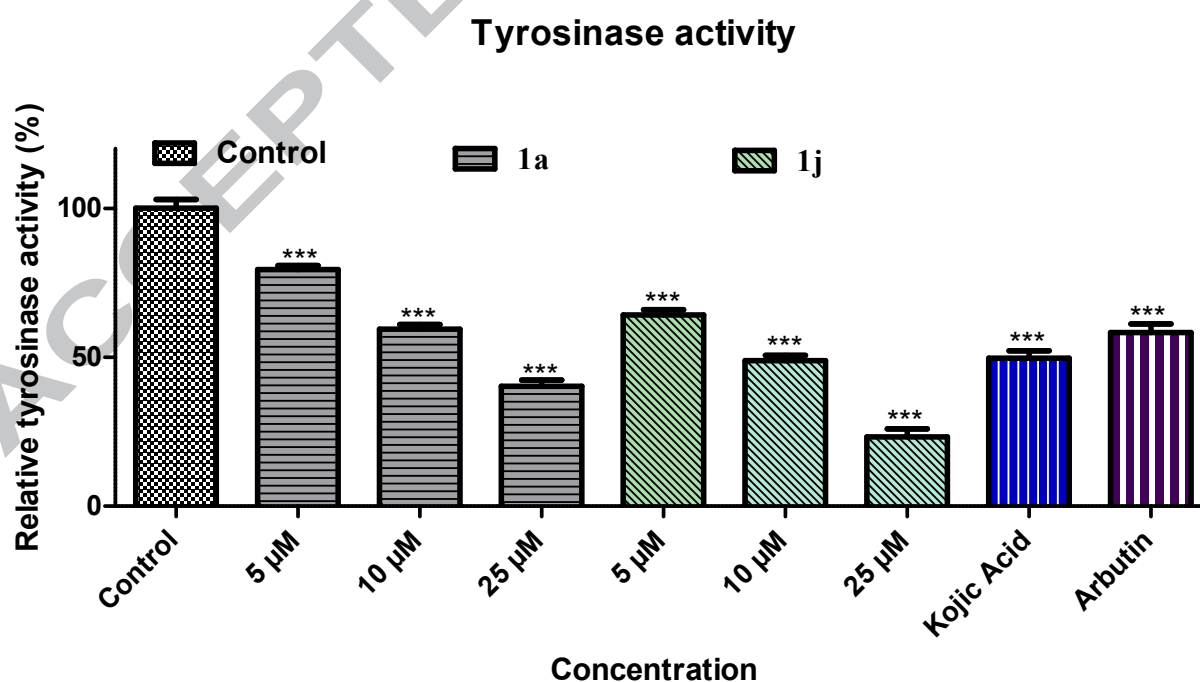


Figure 3. Mammalian tyrosinase inhibition by NAB derivatives **1a** and **1j** in α -MSH stimulated B16F10 melanoma cells. The cells were treated with NAB derivatives **1a** or **1j** (5, 10 or 25 μ M), kojic acid (25 μ M), or arbutin (400 μ M) in the presence of α -MSH. Asterisks indicate significant differences between columns: ***, $p < 0.001$. Standard errors are represented by bars.

*2.6. Melanin content assays of B16F10 melanoma cells treated with NAB derivatives **1a** or **1j***

B16F10 melanoma cells were activated with α -MSH and then treated with **1a**, **1j** (5, 10, or 25 μ M), or kojic acid (25 μ M) and incubated for 24 h. Melanin levels were determined by measuring optical densities.

As indicated in Figure 4, NAB derivatives **1a** and **1j** significantly reduced melanin production versus kojic acid. When treated at concentrations of 5, 10, or 25 μ M, melanin levels reduced by 9.06%, 31.24%, and 47.97%, respectively, for **1a**, and 21.58%, 37.57%, and 61.77% for **1j**. At 25 μ M, kojic acid reduced melanin content by only 38.98%. Somewhat surprisingly, **1j** at 10 μ M reduced melanin levels to the same level as kojic acid at 25 μ M. Because tyrosinase controls the rate-limiting step during melanogenesis, the decrease in melanin content will be closely associated with the inhibition of tyrosinase. As was expected, the melanin contents shown in Figure 4 are similar to the tyrosinase activities depicted in Figure 3.

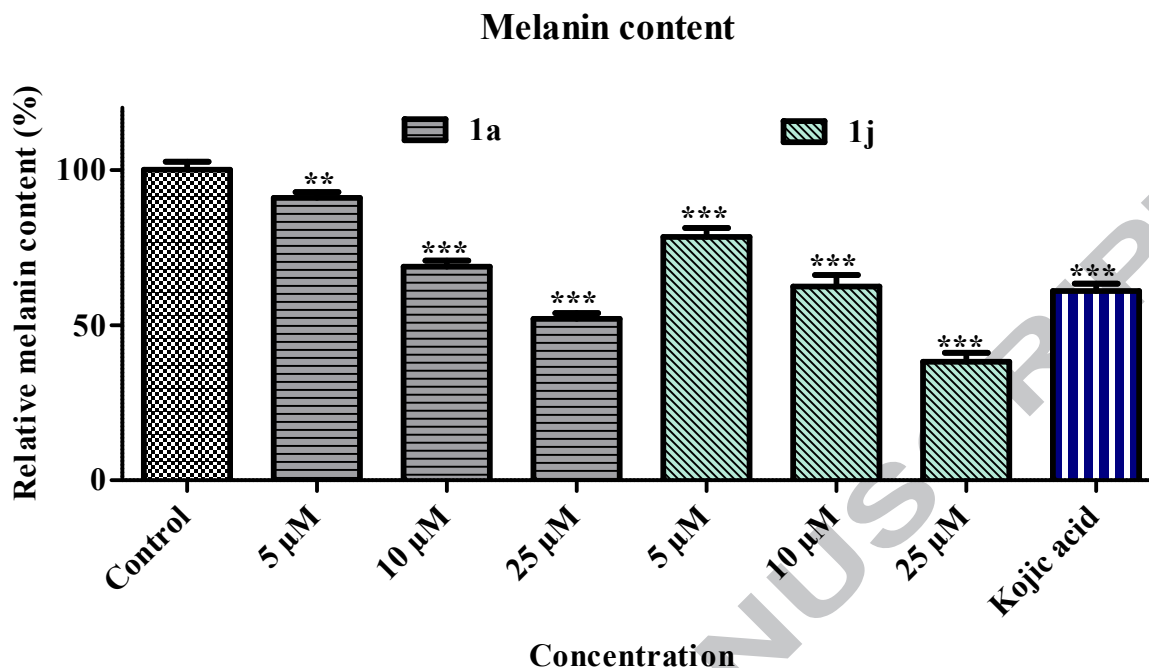


Figure 4. Effects of NAB derivatives **1a** and **1j** on melanin levels in α -MSH stimulated B16F10 melanoma cells. B16F10 melanoma cells were treated with **1a**, **1j** (5, 10 or 25 μ M) or kojic acid (25 μ M). Asterisks indicate significance differences between columns: ***, $p < 0.001$. Standard errors are marked as bars.

2.7. DPPH radical scavenging assay of NAB derivatives **1a** – **1j**

NAB derivatives **1a** – **1j** (1 mM) and L-ascorbic acid were added to a DPPH solution in methanol, and radical scavenging effects were determined 30 min later by measuring percentage absorbances (Table 2).

According to our previously reported structure-activity data on DPPH radical scavenging activity,^{40,41} compounds with a 3,4-dihydroxyl substituent on the β -phenyl ring of the β -phenyl- α,β -unsaturated carbonyl motif usually exhibit high levels of DPPH radical scavenging activity.

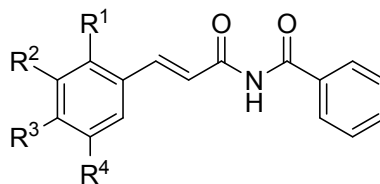
This trend was also observed for NAB derivatives. NAB derivative **1j**, which possessed a 3,4-dihydroxyphenyl substituent, showed greatest DPPH radical scavenging activity $82.89 \pm 0.32\%$,

which was similar to that of L-ascorbic acid ($84.64 \pm 0.32\%$; positive control) (Table 2). The other NAB derivatives did not exhibit prominent radical scavenging effects. ROS (reactive oxygen species) are well known to participate in melanogenesis by mediating the activation of tyrosinase.

Therefore, it is suggested that NAB derivative **1j** may reduce melanin production *in vivo* by the dual mechanism of direct tyrosinase activity inhibition and radical scavenging effect.

Table 2. DPPH radical scavenging activity of NAB derivatives **1a** – **1j** and kojic acid

| Compound | DPPH radical scavenging activity (%) |
|-----------------|--------------------------------------|
| 1a | 7.02 ± 1.32 |
| 1b | 5.61 ± 1.18 |
| 1c | 4.82 ± 0.51 |
| 1d | 5.76 ± 0.65 |
| 1e | 6.90 ± 0.76 |
| 1f | 3.76 ± 0.20 |
| 1g | 17.26 ± 1.11 |
| 1h | NA ^a |
| 1i | 4.89 ± 1.15 |
| 1j | 82.89 ± 0.32 |
| L-Ascorbic acid | 84.64 ± 0.32 |



Radical scavenging was measured at an NAB derivative and an L-ascorbic acid concentration of 1 mM. Three independent experiments were performed and results are expressed as means \pm standard deviations. ^aNA: no activity.

3. Conclusion

In this study, ten NAB derivatives designated **1a** – **1j** were synthesized by the Horner-Wadsworth-Emmons olefination of diethyl (2-benzamido-2-oxoethyl)phosphonate using appropriate benzaldehydes and screened for mushroom tyrosinase inhibition. Of these 10 compounds, **1a** (36.71 \pm 2.14% inhibition), and **1j** (25.99 \pm 2.77% inhibition) inhibited tyrosinase activities to the greatest extents and had also greater inhibitory effects than kojic acid (21.56 \pm 2.93% inhibition). The mushroom tyrosinase inhibitory results obtained were supported by our docking study results, which showed **1a** (-6.9 kcal/mole) and **1j** (-7.5 kcal/mole) bound to tyrosinase stronger than kojic acid (-5.7 kcal/mole). B16F10 melanoma cells were used to investigate the safety profiles of NAB derivatives **1a** and **1j**, and also to determine their effects on cellular tyrosinase activity and cellular melanin contents. According to the results obtained, neither **1a** nor **1j** had a cytotoxic effect on B16F10 melanoma cells at concentrations up to 25 μ M. Furthermore, **1a** and **1j** inhibited tyrosinase more (59.70% and 76.77%, respectively) at 25 μ M than kojic acid (50.30% inhibition at 25 μ M) or arbutin (41.78% inhibition at 400 μ M). Similarly, at 25 μ M **1a** and **1j** reduced melanin contents by 47.97% and 61.77%, respectively, whereas kojic acid only reduced it by 38.98%. The similarity between our tyrosinase and melanin content inhibition results suggests that the anti-melanogenic effects of **1a** and **1j** are mainly due to their tyrosinase inhibitory abilities. Compound **1j** also exhibited potent DPPH

radical scavenging activity ($82.89 \pm 0.32\%$). Collectively, these results imply that **1j** is a promising candidate for the purpose of prevention and treatment of skin hyperpigmentation diseases.

4. Materials and Methods

4.1. Chemistry

Masses of NAB derivatives were obtained by mass spectroscopy. High-resolution mass spectra were recorded on an Agilent Accurate-Mass Q-TOF liquid–chromatography-mass spectrometer (Agilent, Santa Clara, CA, USA). Structure elucidation was performed using a Varian Unity INOVA ^1H NMR and a ^{13}C NMR spectrophotometer (Agilent Technologies, Santa Clara, CA, USA) using $\text{DMSO-}d_6$ and CDCl_3 as solvents. Chemical shifts were measured in ppm (parts per million) against residual solvents or deuterated peaks (for $\text{DMSO-}d_6$, δ_{C} 39.7 and δ_{H} 2.50, and for CDCl_3 , δ_{C} 77.0 and δ_{H} 7.24). Coupling constants were measured in hertz. The following abbreviations are used to present NMR data: s (singlet), brs (broad singlet), d (doublet), dd (doublet of doublets), t (triplet), td (triplet of doublets), q (quartet), qd (quartet of doublets) and m (multiplet). Reaction were monitored by thin layer chromatography (TLC), which was performed using 60 F_{254} glass silica gel plates from Merck. All intermediates and final products were purified by extraction, filtration, and/or MP silica 40 – 63 (60 Å) column chromatography.

4.1.1. Synthesis of *N*-(2-chloroacetyl)benzamide (2). Benzamide (12.10 g, 99.88 mmol) and chloroacetyl chloride (8.20 mL, 103.01 mmol) were added to a 250 mL round-bottomed flask at 0°C, and then refluxed for 50 min. After cooling to room temperature, diethyl ether (30 mL) was added and volatiles were removed under reduced pressure. The precipitate that formed was filtered to obtain **2** as yellowish white solid at a yield of 58%.

¹H NMR (500 MHz, DMSO-*d*₆) δ 11.42 (s, 1H, NH), 7.92 (d, 2H, *J* = 8.0 Hz, 2'-H, 6'-H), 7.63 (t, 1H, *J* = 8.0 Hz, 4'-H), 7.51 (t, 2H, *J* = 8.0 Hz, 3'-H, 5'-H), 4.76 (s, 2H, CH₂); ¹³C NMR (100 MHz, DMSO-*d*₆) δ 169.1, 167.1, 133.7, 133.2, 129.2, 129.1, 46.5.

4.1.2. Synthesis of diethyl (2-benzamido-2-oxoethyl)phosphonate (3). Compound **2** (3.00 g, 15.18 mmol) and triethyl phosphite (6.6 mL, 37.93 mmol) were added to a 100 mL round-bottomed flask and heated at 80°C for 24 h. After cooling, hexane (6.0 mL) was added and the supernatant was removed; this procedure was repeated 5 times. The resulting residue was recrystallized from toluene and hexane (3:1) and the solid generated was filtered to give compound **3**. The filtrate was then evaporated and the residue obtained was purified by silica gel column chromatography using hexane and ethyl acetate (5:1) as eluent to afford additional compound **3**. After recrystallization and column chromatography compound **3** was obtained as a white solid at a yield of 51% (2.294 g). ¹H NMR (500 MHz, CDCl₃) δ 9.85 (s, 1H, NH), 7.93 (d, 2H, *J* = 7.5 Hz, 2'-H, 6'-H), 7.58 (t, 1H, *J* = 7.5 Hz, 4'-H), 7.48 (t, 2H, *J* = 7.5 Hz, 3'-H, 5'-H), 4.17 (qd, 4H, *J* = 7.0, 6.5 Hz, OCH₂CH₃), 3.47 (d, 2H, *J* = 21.5 Hz, PCH₂), 1.32 (t, 6H, *J* = 7.0 Hz, OCH₂CH₃); ¹³C NMR (100 MHz, CDCl₃) δ 165.5, 165.3, 133.5, 132.7, 129.2, 128.1, 63.3 (d, *J* = 6.8 Hz), 36.7 (d, *J* = 129.8 Hz), 16.5 (d, *J* = 6.1 Hz).

4.1.3. General procedure for the syntheses of compounds 4 and 5. 4-Hydroxybenzaldehyde (2.00 g, 16.38 mmol) or 3,4-dihydroxybenzaldehyde (3.00 g, 21.72 mmol), pyridinium *p*-

toluenesulfonate (0.02 equiv.), and DCM (20 mL/g of benzaldehyde) were added to a 250 mL round-bottomed flask. A solution of 3,4-dihydro-2*H*-pyran (4.5 mL, 49.32 mmol for 4-hydroxybenzaldehyde and 9.9 mL, 108.5 mmol of 3,4-dihydroxybenzaldehyde) in DCM (25 mL) was then added and the reaction mixture was stirred at room temperature for 2 – 50 h. After reaction completion, the reaction mixture was partitioned between DCM and saturated aqueous NaHCO₃ solution, and the organic layer was dried over MgSO₄, filtered, and evaporated under reduced pressure. The resultant residue was purified by silica gel column chromatography using hexane and ethyl acetate (9:1 for **4**, and 4:1 for **5**) to afford compound **4** (3.069 g, 90.9%) and compound **5** (5.32 g, 79.7%), respectively. Compound **5** was used immediately in the next reaction without the structural analysis.

4-((Tetrahydro-2*H*-pyran-2-yl)oxy)benzaldehyde (4**).** Yellowish white solid, 91% yield. ¹H NMR (400 MHz, CDCl₃) δ 9.87 (s, 1H, CHO), 7.80 (d, 2H, *J* = 8.8 Hz, 2-H, 6-H), 7.13 (d, 2H, *J* = 8.8 Hz, 3-H, 5-H), 5.52 (t, 1H, *J* = 2.8 Hz, 2'-H), 3.82 (td, 1H, *J* = 11.2, 2.8 Hz, 6'-Ha), 3.63 – 3.58 (m, 1H, 6'-Hb), 2.01 – 1.94 (m, 1H), 1.88 – 1.85 (m, 2H), 1.71 – 1.65 (m, 2H), 1.61 – 1.57 (m, 1H); ¹³C NMR (100 MHz, CDCl₃) δ 191.2, 162.3, 132.1, 130.6, 116.7, 96.3, 62.3, 30.2, 25.2, 18.6.

4.1.4. General procedure for the syntheses of compounds **6 and **7**.** A solution of **3** (118 mg, 0.39 mmol for **6**, or 181 mg, 0.60 mmol for **7**) in THF (2.5 mL) and a solution of **4** (81.4 mg, 0.39 mmol) or **5** (185 mg, 0.60 mmol) in THF (2.5 mL) were added to a stirred suspension of NaH (60% in mineral oil, 39.4 mg, 0.99 mmol for **6**, or 72.5 mg, 1.81 mmol for **7**) in THF (2.5 mL). The reaction mixture was then stirred at room temperature for 3 h, and saturated NH₄Cl aqueous solution was added. For the synthesis of **6**, water was added and the precipitate generated was filtered to give **6** (95.3 mg, 68.8%) as a yellow solid. For the synthesis of **7**, the

reaction mixture was partitioned between DCM and water, and the filtrate was dried over MgSO₄, filtered, and evaporated under reduced pressure to give crude compound **7** (240.3 mg, 88.1%), which was immediately used in the next step without the structural analysis.

(E)-N-(3-(4-((Tetrahydro-2H-pyran-2-yl)oxy)phenyl)acryloyl)benzamide (6). ¹H NMR (400 MHz, CDCl₃) δ 8.70 (s, 1H, NH), 7.88 (d, 2H, J = 8.8 Hz, 2'-H, 6'-H), 7.87 (d, 1H, J = 15.6 Hz, β -vinylic H), 7.71 (d, 1H, J = 15.6 Hz, α -vinylic H), 7.61 – 7.56 (m, 3H, 2-H, 4-H, 6-H), 7.49 (t, 2H, J = 8.0 Hz, 3-H, 5-H), 7.04 (d, 2H, J = 8.8 Hz, 3'-H, 5'-H), 5.46 (t, 1H, J = 2.8 Hz, 2'-H), 3.85 (td, 1H, J = 11.2, 2.8 Hz, 6'-Ha), 3.63 – 3.57 (m, 1H, 6'-Hb), 2.03 – 1.94 (m, 1H), 1.88 – 1.84 (m, 2H), 1.70 – 1.64 (m, 2H), 1.61 – 1.57 (m, 1H); ¹³C NMR (100 MHz, CDCl₃) δ 168.0, 166.0, 159.5, 146.9, 133.4, 130.6, 129.2, 128.3, 127.9, 117.1, 116.9, 96.3, 62.2, 30.4, 25.3, 18.8.

4.1.5. General procedure for the syntheses of NAB derivatives 1a – 1h. Anhydrous THF (3 mL) and sodium hydride (2.5 equiv., 60% in mineral oil) were added to a 25 mL round-bottomed flask, and then a solution of compound **3** (100 mg, 0.33 mmol) in THF (1.0 mL), and a solution of appropriate benzaldehyde (1.0 equiv.) in THF (1.0 mL) were added. After stirring at room temperature for 1 – 12 h, aqueous ammonium chloride solution was added at 0 °C. The precipitates generated were filtered and the filter cake so obtained was washed with water and dried to obtain the NAB derivatives **1a – 1h** as solids in yields of 26 – 86%.

(E)-N-(3-(3-Hydroxy-4-methoxyphenyl)acryloyl)benzamide (1a). Yellowish white solid, 49% yield. ¹H NMR (400 MHz, DMSO-*d*₆) δ 11.00 (s, 1H, NH), 9.29 (s, 1H, OH), 7.89 (d, 2H, J = 8.4 Hz, 2-H, 6-H), 7.60 (t, 1H, J = 8.0 Hz, 4-H), 7.55 (d, 1H, J = 15.2 Hz, β -vinylic H), 7.50 (t, 2H, J = 8.0 Hz, 3-H, 5-H), 7.10 (d, 1H, J = 15.2 Hz, α -vinylic H), 7.07 (s, 1H, 2''-H), 7.06 (d, 1H, J = 8.0 Hz, 6''-H), 6.94 (d, 1H, J = 8.0 Hz, 5''-H), 3.78 (s, 3H, OCH₃); ¹³C NMR (100 MHz,

DMSO- d_6) δ 167.3, 166.7, 150.8, 147.4, 144.6, 134.2, 133.4, 129.2, 129.0, 127.9, 122.3, 118.9, 114.2, 112.7, 56.3; HRMS (ESI+) m/z $C_{17}H_{16}NO_4$ (M+H)⁺ calcd 298.1074, obsd 298.1072, $C_{17}H_{15}NNaO_4$ (M+Na)⁺ calcd 320.0893, obsd 320.0894.

(E)-N-(3-(4-Methoxyphenyl)acryloyl)benzamide (1b). Yellow solid, 73% yield. ¹H NMR (400 MHz, DMSO- d_6) δ 11.03 (s, 1H, NH), 7.90 (d, 2H, J = 8.0 Hz, 2-H, 6-H), 7.65 (d, 1H, J = 15.6 Hz, β -vinylic H), 7.60 (d, 2H, J = 8.8 Hz, 2'-H, 6'-H), 7.59 (t, 1H, J = 8.0 Hz, 4-H), 7.50 (t, 2H, J = 8.0 Hz, 3-H, 5-H), 7.17 (d, 1H, J = 15.6 Hz, α -vinylic H), 6.99 (d, 2H, J = 8.8 Hz, 3'-H, 5'-H), 3.77 (s, 3H, OCH₃); ¹³C NMR (100 MHz, DMSO- d_6) δ 167.3, 166.8, 161.8, 144.1, 134.2, 133.4, 130.6, 129.2, 129.0, 127.7, 119.2, 115.2, 56.0; HRMS (ESI+) m/z $C_{17}H_{16}NO_3$ (M+H)⁺ calcd 282.1125, obsd 282.1127, $C_{17}H_{15}NNaO_3$ (M+Na)⁺ calcd 304.0944, obsd 304.0946.

(E)-N-(3-(3,4-Dimethoxyphenyl)acryloyl)benzamide (1c). Yellowish white solid, 77% yield. ¹H NMR (400 MHz, CDCl₃) δ 8.73 (s, 1H, NH), 7.88 (d, 1H, J = 7.6 Hz, 2-H, 6-H), 7.86 (d, 1H, J = 15.6 Hz, β -vinylic H), 7.70 (d, 1H, J = 15.6 Hz, α -vinylic H), 7.60 (t, 1H, J = 7.6 Hz, 4-H), 7.45 (t, 2H, J = 7.6 Hz, 3-H, 5-H), 7.19 (dd, 2H, J = 8.4, 1.6 Hz, 6'-H), 7.15 (d, 1H, J = 1.6 Hz, 2'-H), 6.86 (d, 1H, J = 8.4 Hz, 5'-H), 3.92 (s, 3H, OCH₃), 3.90 (s, 3H, OCH₃); ¹³C NMR (100 MHz, CDCl₃) δ 167.9, 166.2, 151.8, 149.4, 147.2, 133.4, 133.3, 129.2, 127.9, 127.9, 123.9, 117.0, 111.1, 110.1, 56.2, 56.2; HRMS (ESI+) m/z $C_{18}H_{18}NO_4$ (M+H)⁺ calcd 312.1230, obsd 312.1225, $C_{18}H_{17}NNaO_4$ (M+Na)⁺ calcd 334.1050, obsd 334.1052.

(E)-N-(3-(2,4-Dimethoxyphenyl)acryloyl)benzamide (1d). White solid, 86% yield. ¹H NMR (500 MHz, CDCl₃) δ 8.68 (s, 1H, NH), 8.22 (d, 1H, J = 16.0 Hz, β -vinylic H), 7.90 (d, 2H, J = 7.5 Hz, 2-H, 6-H), 7.80 (d, 1H, J = 16.0 Hz, α -vinylic H), 7.62 (d, 1H, J = 8.5 Hz, 6'-H), 7.61 (t, 1H, J = 7.5 Hz, 4-H), 7.51 (t, 2H, J = 7.5 Hz, 3-H, 5-H), 6.52 (dd, 1H, J = 8.5, 2.5 Hz, 5'-H),

6.46 (d, 1H, $J = 2.5$ Hz, 3'-H), 3.90 (s, 3H, OCH₃), 3.86 (s, 3H, OCH₃); ¹³C NMR (100 MHz, CDCl₃) δ 168.4, 166.1, 163.5, 160.5, 142.5, 133.6, 133.2, 131.1, 129.2, 127.9, 117.1, 116.9, 105.6, 98.5, 55.8, 55.7; HRMS (ESI+) m/z C₁₈H₁₈NO₄ (M+H)⁺ calcd 312.1230, obsd 312.1235, C₁₈H₁₇NNaO₄ (M+Na)⁺ calcd 334.1050, obsd 334.1053.

(E)-N-(3-(3,4,5-Trimethoxyphenyl)acryloyl)benzamide (1e). Yellowish White solid, 73% yield. ¹H NMR (400 MHz, CDCl₃) δ 8.68 (s, 1H, NH), 7.88 (d, 2H, $J = 7.6$ Hz, 2-H, 6-H), 7.83 (d, 1H, $J = 15.6$ Hz, β -vinylic H), 7.72 (d, 1H, $J = 15.6$ Hz, α -vinylic H), 7.60 (t, 1H, $J = 7.2$ Hz, 4-H), 7.50 (t, 2H, $J = 7.6$ Hz, 3-H, 5-H), 6.84 (s, 2H, 2'-H, 6'-H), 3.89 (s, 6H, 2 \times OCH₃), 3.88 (s, 3H, OCH₃); ¹³C NMR (100 MHz, CDCl₃) δ 167.7, 166.1, 153.6, 147.2, 140.8, 133.5, 133.2, 130.3, 129.3, 127.9, 118.6, 106.0, 61.2, 56.4; HRMS (ESI+) m/z C₁₉H₂₀NO₅ (M+H)⁺ calcd 342.1336, obsd 342.1332, C₁₉H₁₉NNaO₅ (M+Na)⁺ calcd 364.1155, obsd 364.1149.

(E)-N-(3-(4-Hydroxy-3,5-dimethoxyphenyl)acryloyl)benzamide (1f). Yellowish White solid, 26% yield. ¹H NMR (400 MHz, DMSO-*d*₆) δ 7.90 (d, 2H, $J = 7.6$ Hz, 2-H, 6-H), 7.60 (d, 1H, $J = 14.8$ Hz, β -vinylic H), 7.60 (t, 1H, $J = 7.6$ Hz, 4-H), 7.50 (t, 2H, $J = 7.6$ Hz, 3-H, 5-H), 7.08 (d, 1H, $J = 14.8$ Hz, α -vinylic H), 6.93 (s, 2H, 2'-H, 6'-H), 3.77 (s, 6H, 2 \times OCH₃); ¹³C NMR (100 MHz, DMSO-*d*₆) δ 167.2, 166.7, 148.8, 145.2, 139.4, 134.3, 133.3, 129.1, 129.0, 125.1, 118.4, 106.7, 56.6; HRMS (ESI+) m/z C₁₈H₁₈NO₅ (M+H)⁺ calcd 328.1179, obsd 328.1174, C₁₈H₁₇NNaO₅ (M+Na)⁺ calcd 350.0999, obsd 350.0994.

(E)-N-(3-(3-Bromo-4-hydroxyphenyl)acryloyl)benzamide (1g). Yellow solid, 32% yield. ¹H NMR (400 MHz, DMSO-*d*₆) δ 10.98 (s, 1H), 10.85 (s, 1H), 7.88 (d, 2H, $J = 8.0$ Hz, 2-H, 6-H), 7.78 (d, 1H, $J = 2.0$ Hz, 2'-H), 7.58 (dd, 1H, $J = 8.4, 2.0$ Hz, 6'-H), 7.55 (d, 1H, $J = 16.0$ Hz, β -

vinyllic H), 7.50 – 7.45 (m, 3H, 3-H, 4-H, 5-H), 7.11 (d, 1H, $J = 16.0$ Hz, α -vinyllic H), 6.96 (d, 1H, $J = 8.4$ Hz, 5'-H); ^{13}C NMR (100 MHz, DMSO- d_6) δ 167.3, 166.5, 156.8, 142.7, 133.4, 133.3, 129.6, 129.1, 129.0, 128.1, 128.0, 119.8, 117.3, 115.3; HRMS (ESI+) m/z $\text{C}_{16}\text{H}_{12}\text{BrNNaO}_3$ (M+Na) $^+$ calcd 367.9893, obsd 367.9889, $\text{C}_{16}\text{H}_{12}\text{BrNNaO}_3$ (M+2+Na) $^+$ calcd 369.9874, obsd 369.9871.

(E)-N-(3-(3,5-Dibromo-4-hydroxyphenyl)acryloyl)benzamide (1h). Yellowish White solid, 32% yield. ^1H NMR (400 MHz, DMSO- d_6) δ 10.82 (brs, 1H), 7.88 (d, 2H, $J = 7.6$ Hz, 2-H, 6-H), 7.67 (s, 2H, 2'-H, 6'-H), 7.59 (t, 1H, $J = 7.6$ Hz, 4-H), 7.49 (t, 2H, $J = 7.6$ Hz, 3-H, 5-H), 7.46 (d, 1H, $J = 16.0$ Hz, β -vinyllic H), 6.94 (d, 1H, $J = 16.0$ Hz, α -vinyllic H); ^{13}C NMR (100 MHz, DMSO- d_6) δ 167.1, 166.6, 159.4, 142.9, 134.3, 133.3, 132.7, 129.1, 128.9, 122.8, 116.2, 114.5; HRMS (ESI+) m/z $\text{C}_{16}\text{H}_{12}\text{Br}_2\text{NO}_3$ (M+H) $^+$ calcd 423.9178, obsd 423.9174, (M+2+H) $^+$ calcd 425.9159, obsd 425.9150, (M+4+H) $^+$ calcd 427.9141, obsd 427.9136, $\text{C}_{16}\text{H}_{11}\text{Br}_2\text{NNaO}_3$ (M+Na) $^+$ calcd 445.8998, obsd 445.8994, (M+2+Na) $^+$ calcd 447.8978, obsd 447.8978, (M+4+Na) $^+$ calcd 449.8960, obsd 44.8955.

4.1.6. General procedure for the syntheses of compounds 1i and 1j. 2M-HCl solution (2.0 mL) was added to a solution of **6** (64 mg, 0.18 mmol) or **7** (342 mg, 0.76 mmol) in 1,4-dioxane (2.0 mL). The reaction mixture was stirred at room temperature for 30 min for **1i** and for 6 h for **1j**. For **1i**, the reaction mixture was partitioned between DCM and water, and the aqueous layer was filtered to give **1i**. In addition, the organic layer was evaporated under reduced pressure, hexane was added to the residue, and the resulting precipitate was filtered to give **1i** (30.6 mg, yield 62.9%) as a yellow solid. For **1j**, after adding water, the precipitate was filtered and washed with water to afford **1j** (105.9 mg, 49.3%) as a yellowish white solid.

(E)-N-(3-(4-Hydroxyphenyl)acryloyl)benzamide (1i). ^1H NMR (400 MHz, DMSO- d_6) δ 10.98 (s, 1H, NH), 10.05 (s, 1H, OH), 7.89 (d, 2H, $J = 7.6$ Hz, 2-H, 6-H), 7.61 (d, 1H, $J = 16.0$ Hz, β -vinyllic H), 7.60 (t, 1H, $J = 7.6$ Hz, 4-H), 7.50 (t, 2H, $J = 7.6$ Hz, 3-H, 5-H), 7.48 (d, 2H, $J = 8.4$ Hz, 2'-H, 6'-H), 7.10 (d, 1H, $J = 16.0$ Hz, α -vinyllic H), 6.80 (d, 2H, $J = 8.4$ Hz, 3'-H, 5'-H); ^{13}C NMR (100 MHz, DMSO- d_6) δ 167.3, 166.8, 160.5, 144.6, 134.2, 133.3, 130.9, 129.1, 129.0, 126.2, 118.0, 116.6; HRMS (ESI+) m/z $\text{C}_{16}\text{H}_{14}\text{NO}_3$ (M+H) $^+$ calcd 268.0968, obsd 268.0969, $\text{C}_{16}\text{H}_{13}\text{NNaO}_3$ (M+Na) $^+$ calcd 290.0788, obsd 290.0787.

(E)-N-(3-(3,4-Dihydroxyphenyl)acryloyl)benzamide (1j). ^1H NMR (400 MHz, DMSO- d_6) δ 10.96 (s, 1H, NH), 9.58 (brs, 1H, OH), 9.24 (brs, 1H, OH), 7.89 (d, 2H, $J = 7.6$ Hz, 2-H, 6-H), 7.60 (t, 1H, $J = 7.6$ Hz, 4-H), 7.53 (d, 1H, $J = 15.4$ Hz, β -vinyllic H), 7.50 (t, 2H, $J = 7.6$ Hz, 3-H, 5-H), 7.07 (d, 1H, $J = 15.6$ Hz, α -vinyllic H), 7.04 (d, 1H, $J = 2.0$ Hz, 2'-H), 6.94 (dd, 1H, $J = 8.0, 2.0$ Hz, 6'-H), 6.75 (d, 1H, $J = 8.0$ Hz, 5'-H); ^{13}C NMR (100 MHz, DMSO- d_6) δ 167.3, 166.9, 149.2, 146.3, 145.1, 134.3, 133.3, 129.1, 129.0, 126.6, 122.5, 117.8, 116.5, 114.8; HRMS (ESI+) m/z $\text{C}_{16}\text{H}_{14}\text{NO}_4$ (M+H) $^+$ calcd 284.0917, obsd 284.0909, $\text{C}_{16}\text{H}_{13}\text{NNaO}_4$ (M+Na) $^+$ calcd 306.0737, obsd 306.0718.

4.2. Docking simulation for NAB derivatives 1a and 1j

Docking simulations for **1a**, **1j**, and kojic acid were carried out as previously described.⁴²⁻⁴⁴ Chem3D Pro 12.0 software was used to generate the 3D structures of **1a** and **1j**. AutoDock Vina and Chimera software were used to calculate binding scores between tyrosinase and the two derivatives and kojic acid. The three-dimensional structure of tyrosinase (*Agaricus Bisporus*) was obtained from the Protein Data Bank (PDB ID: 2Y9X). LigandScout software 4.3.0 was

used to generate pharmacophore models showing possible interactions between the three ligands and the amino acid residues of tyrosinase.

4.3. Biological Evaluation

4.3.1. Mushroom tyrosinase inhibition assays of NAB derivatives **1a – 1j**

To determine the mushroom tyrosinase inhibition activities of NAB derivatives, we used a slight modification of a previously described procedure.⁴⁵ NAB derivatives (**1a – 1j**, 10 μ L, 25 μ M) and 20 μ L of tyrosinase solution (one thousand units per mL) were added to the 170 μ L solution of 14.7 mM phosphate buffer containing 293 μ M of L-tyrosine in the wells of a 96-well plate and incubated for 30 min at 37°C. Percentage tyrosinase inhibition was determined by measuring optical densities at 450 nm using a shaking microplate reader (VersaMax). Kojic acid (25 μ M) was used as the control. The experiments were repeated three times. The formula used to calculate % inhibition was;

$$\% \text{Inhibition} = 100 \times [1 - (A/B)]$$

where A is sample absorbance and B is the absorbance of blank control (non-treated).

4.3.2. Cell culture

The B16F10 murine melanoma cells used for cell viability, tyrosinase inhibition, and melanin content assays were obtained from the American Type Culture Collection (ATCC, VA, USA) and cultured in DMEM (Dulbecco's medium) containing 10% foetal bovine serum (FBS), 100 μ g/mL streptomycin, and 100 IU/ml penicillin in a humidified 5% CO₂ atmosphere at 37°C.

4.3.3. Cell viability assay

The cell viabilities of NAB derivatives **1a** and **1j** were determined using a WST-8 assay, as previously described.⁴⁶ B16F10 murine melanoma cells (5×10^4 cells per well) were incubated at 37 °C for 24 h in a humidified 5% CO₂ atmosphere in 96-well plates. Compounds **1a** and **1j** at concentrations of 0, 5, 10, or 25 were added, and cells were re-incubated for 24 h under the same conditions. On the following day, cells were treated with WST-8 reagents and incubated for 30 min at 37°C for 2 h 30 min later, and viabilities were determined using an EZ-Cytox assay (EZ-3000, Daeil Lab Service, Seoul) by reading optical densities at 450 nm. Experiments were repeated three times.

4.3.4. Tyrosinase inhibition assay

Tyrosinase inhibition assays of NAB derivatives **1a** and **1j** were performed as previously described with slight changes.⁴⁷ In brief, B16F10 cells were inoculated at 5×10^4 cells per well in 96-well plates and incubated for 24 h in a humidified 5% CO₂ atmosphere at 37 °C. The cells were then treated with α -MSH (1 μ M) and kojic acid (25 μ M) or α -MSH (1 μ M) and **1a** or **1j** (0, 5, 10, or 25 μ M) and re-cultured for 24 h under the same conditions. Cells were then washed with PBS buffer, lysed with lysis buffer (100 μ L containing 1% Triton X-100 (5 μ L), 0.1 mM PMSF (5 μ L), and 50 mM PBS (pH 6.8, 90 μ L), frozen at -80 °C for 30 min, centrifuged at 12,000 rpm for 30 min at 4°C, transferred to 96-well plates, treated with L-dopa (total volume 100 μ L; 80 μ L of supernatant and 20 μ L of 10 mM L-dopa), and incubated for 30 min at 37°C. Tyrosinase inhibitions were determined by measuring optical densities at 500 nm in a Tecan, Mannedorf microplate reader. The experiment was performed in triplicate.

4.3.5. Anti-melanogenic assay

The anti-melanogenic effects of NAB derivatives **1a** and **1j** were determined by measuring melanin contents, as previously described with slight changes.⁴⁸ Briefly, B16F10 cells were inoculated at 5×10^4 cells per well in 96-well plates and incubated for 24 h in a humidified 5% CO₂ atmosphere at 37 °C. Cells were then treated with α -MSH (1 μ M) and kojic acid (25 μ M) or with α -MSH (1 μ M) and NAB derivatives **1a** or **1j** (0, 5, 10, or 25 μ M) and re-cultured for 24 h as described above. Cells were then washed twice with PBS buffer and treated with 1M-NaOH aqueous solution (200 μ L) for 1 h to dissolve melanin. Solutions were transferred to 96-well plates and melanin contents were determined by measuring optical densities at 405 nm in a Tecan, Mannedorf microplate reader. The experiment was performed in triplicate.

4.3.6. DPPH radical scavenging assay

To determine the antioxidant activities of NAB derivatives **1a** – **1j**, a DPPH radical scavenging assay was performed as previously described with a few changes.⁴⁹ In summary, 20 μ L of a DMSO solution of each NAB derivative (10 mM) was mixed with 180 μ L of DPPH solution (0.2 mM) in methanol in 96-well plates. L-Ascorbic acid was used as a positive control. Mixtures were then incubated for 30 min in the dark, and antioxidant activities were determined by measuring absorbances at 517 nm using a VersaMax microplate reader. The experiments were performed in triplicate. The formula used to determine DPPH radical scavenging activity was as follows:

$$\text{Radical scavenging activity (\%)} = 100 \times [(Ac-As)/Ac]$$

Where Ac is the absorbance of the non-treated control, and As is the absorbance of a sample or a L-ascorbic acid treated solution.

4.3.7. Statistical analysis

Statistical analysis was performed using GraphPad Prism 5 software (La Jolla, CA, USA). All experiments were performed in triplicate. Results are expressed as means \pm SEMs. One-way ANOVA and Tukey's test were used to determine the significances of intergroup differences. *P*-values were considered to be statistically significant.

Acknowledgment

This research was supported by the Basic Science Research Program through the National Research Foundation of Korea (NRF) funded by the Ministry of Education (NRF-2017R1D1A1B03027888).

References

1. Bonaventure J, Domingues MJ, Larue L. *Pigment cell & Melanoma Res.* 2013;26:316-325.
2. Decker H, Schweikardt T, Tuzcek F. *Ang Chemie Intl Ed.* 2006;45:4546-4550.
3. Ahn SJ, Koketsu M, Ishihara H, et al. *Chem Pharm Bull.* 2006;54:281-286.
4. Artés F, Castaner M, Gil M. *Food Sci Tech Intl.* 1998;4:377-389.
5. Bae SJ, Ha YM, Park YJ, et al. *Eur J Med Chem.* 2012;57:383-390.
6. Ramsden CA, Riley PA. *Arkivoc.* 2010;1:260-274.
7. Ramsden CA, Stratford MR, Riley PA. *Organic & Biomolecular Chem.* 2009;7:3388-3390.
8. Sánchez-Ferrer A, Rodríguez-López JN, García-Cánovas F, García-Carmona F. *BBA.* 1995;1247:1-11.
9. Muñoz-Muñoz J, Acosta-Motos J, Garcia-Molina F, et al. *BBA.* 2010;1804:1467-1475.
10. Agarwal KC. Mechanism-based biochemical standardization of resveratrol products and their uses thereof. US6414037B1; 2011.
11. Kidson S, De Haan J. *Exp Cell Res.* 1990;188:36-41.
12. Imokawa G. *The J Invest dermatol.* 1989;93:100-107.

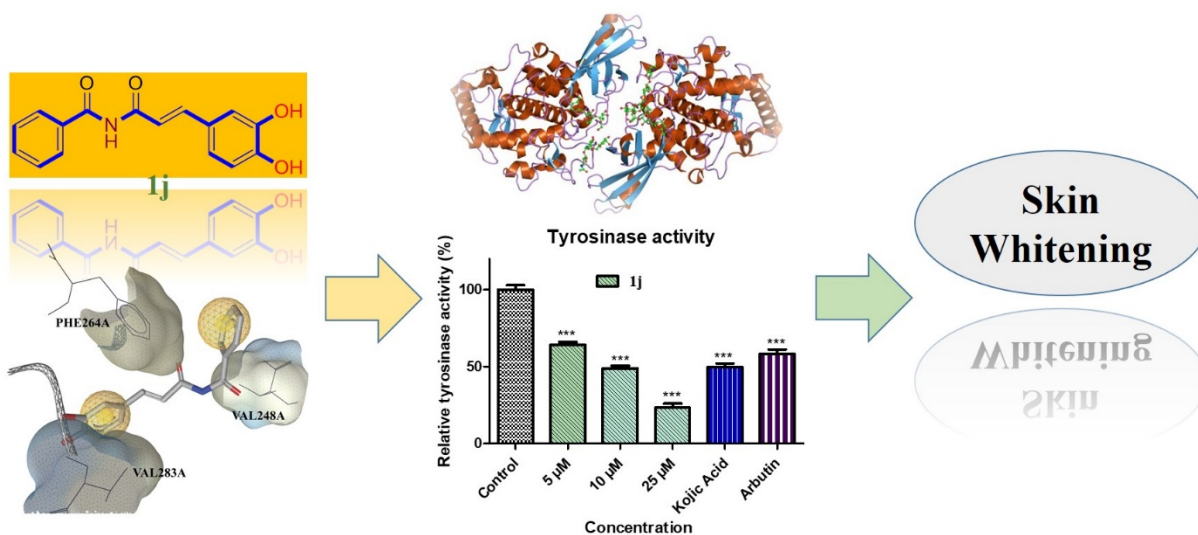
13. Petrescu SM, Branza-Nichita N, Negroiu G, Petrescu AJ, Dwek RA. *Biochemistry*. 2000;39:5229-5237.
14. Saeki H, Oikawa A. *J Cellular physiol*. 1980;104:171-175.
15. Ando H, Kondoh H, Ichihashi M, Hearing VJ. *The J Invest dermatol*. 2007;127:751-761.
16. Kumar KS, Vani MG, Wang SY, et al. *Biofactors*. 2013;39:259-270.
17. Arndt KA, Fitzpatrick TB. *JAMA*. 1965;194:965-967.
18. Fitzpatrick T, Arndt K, El Mofty A, Pathak M. *Archi Dermatol*. 1966;93:589-600.
19. Heiligemeir G, Balda B. *MMW, Munch Med Woch*. 1981;123:47.
20. Kligman AM, Willis I. *Archi Dermatol*. 1975;111:40-48.
21. Gonçalves M, Correa MA, Chorilli M. *BioMed Res Intl*. 2013;2013.
22. Breathnach AC, Nazzaro-Porro M, Passi S, Zina G. *Clinics in Dermatol*. 1989;7:106-119.
23. Garcia-Lopez M. *Acta Derm Venereol (Stockh)*. 1989;143:58-61.
24. Curto EV, Kwong C, Hermersdörfer H, et al. *Biochem Pharmacol*. 1999;57:663-672.
25. Engasser PG. *J A A Dermatol*. 1984;10:1072-1073.
26. Fisher A. *Cutis*. 1983;31:240-244, 250.
27. Romaguera C, Grimalt F. *Contact Dermatitis*. 1985;12:183-183.
28. Barcelos RC, Pastre JC, Vendramini-Costa DB, et al. *ChemMedChem*. 2014;9:2725-2743.
29. Gunia-Krzyżak A, Żelaszczyk D, Rapacz A, et al. *Bioorg Med Chem*. 2017;25:471-482.
30. Spasova M, Kortenska-Kancheva V, Totseva I, Ivanova G, Georgiev L, Milkova T. *J Peptide Sci: an official publication of the European Peptide Society*. 2006;12:369-375.
31. Spasova M, Philipov S, Nikolaeva-Glomb L, Galabov A, Milkova T. *Bioorg Med Chem*. 2008;16:7457-7461.
32. Georgiev L, Chochkova M, Totseva I, et al. *Med Chem Res*. 2013;22:4173-4182.
33. Sova M. *Mini Reviews in Med Chem*. 2012;12:749-767.
34. Bandgar BP, Adsul LK, Chavan HV, et al. *Bioorg Med Chem*. 2012;20:5649-5657.
35. Kavala V, Wang C-C, Barange DK, Kuo C-W, Lei P-M, Yao C-F. *JOC*. 2012;77:5022-5029.
36. Romagnoli R, Prencipe F, Lopez-Cara LC, et al. *J Enz Inhi Med Chem*. 2018;33:727-742.
37. Fiorino F, Eiden M, Giese A, et al. *Bioorg Med Chem*. 2012;20:5001-5011.
38. Goodman SN, Jacobsen EN. *Adv Syn Cat*. 2002;344:953-956.
39. Vanderwal CD, Jacobsen EN. *JACS*. 2004;126:14724-14725.
40. Do Hyun Kim SJK, Ullah S, Yun HY, Chun P, Moon HR. *Drug Des Devel Ther*. 2017;11:827.
41. Kim SJ, Yang J, Lee S, et al. *Bioorg Med Chem*. 2018.
42. Morris GM, Goodsell DS, Halliday RS, et al. *J Comp Chem*. 1998;19:1639-1662.
43. Moustakas DT, Lang PT, Pegg S, et al. *J Comput Aided Mol Des*. 2006;20:601-619.
44. Bagherzadeh K, Shirgahi Talari F, Sharifi A, Ganjali MR, Saboury AA, Amanlou M. *J Biomol Struct Dyn*. 2015;33:487-501.
45. Hyun SK, Lee W-H, Jeong DM, Kim Y, Choi JS. *Biol Pharm Bull*. 2008;31:154-158.
46. Ishiyama M, Tominaga H, Shiga M, Sasamoto K, Ohkura Y, Ueno K. *Biol Pharm Bull*. 1996;19:1518-1520.
47. Bae SJ, Ha YM, Kim J-A, et al. *BBA*. 2013;77:65-72.

48. Chen L-G, Chang W-L, Lee C-J, Lee L-T, Shih C-M, Wang C-C. *Biol Pharm Bull.* 2009;32:1447-1452.
49. Matos M, Varela C, Vilar S, et al. *RSC Adv.* 2015;5:94227-94235.

Inhibitory effects of *N*-(acryloyl)benzamide derivatives on tyrosinase and melanogenesis

Sanggwon Lee^{a,§}, Sultan Ullah^{a,§}, Chaeun Park^{a,§}, Hee Won Lee^a, Dongwan Kang^a, Jungho

Yang^a, Jinia Akter^a, Yujin Park^a, Pusoon Chun^b, Hyung Ryong Moon^{a,*}



Highlights

- Ten NAB derivatives were synthesized via Horner-Wadsworth-Emmons olefination.
- **1a** and **1j** exhibited potent anti-melanogenic effects compared to kojic acid.
- **1a** and **1j** showed stronger binding affinities for tyrosinase than kojic acid.

ACCEPTED MANUSCRIPT